

Doubly excited ferromagnetic spin-chain as a pair of coupled kicked rotors

T. Boness,¹ K. Kudo,² and T.S. Monteiro¹

¹*Department of Physics and Astronomy, University College London,
Gower Street, London WC1E 6BT, United Kingdom*

²*Division of Advanced Sciences, Ochanai Academic Production,
Ochanomizu University, 2-1-1 Ohtsuka, Bunkyo-ku, Tokyo 112-8610, Japan*

(Dated: October 30, 2018)

We show that the dynamics of a doubly-excited Heisenberg spin-chain, subject to short pulses from a parabolic magnetic field may be analyzed as a pair of quantum kicked rotors. By focusing on the two-magnon dynamics in the kicked XXZ model we investigate how the anisotropy parameter - which controls the strength of the magnon-magnon interaction - changes the nature of the coupling between the two “image” coupled Kicked Rotors. We investigate quantum state transfer possibilities and show that one may control whether the spin excitations are transmitted together, or separate from each other.

PACS numbers: 75.10.Pq, 03.67.Hk, 05.45.Mt

I. INTRODUCTION

Over recent years, there has been sustained interest in coupled quantum systems. Numerous studies investigated the causes and effects of decoherence on a subsystem as it becomes entangled with its environment; others probed the generation of bipartite entanglement between a pair of quantum systems. It is vitally important to understand these processes so they can be accounted for in protocols for quantum computation and communication.

Studies of decoherence also shed light on the emergence of classical behavior from quantum dynamics [1, 2]. Quantum systems with a chaotic classical limit often feature in such studies. For example, they can play the role of the environment: a 1D system which displays chaos can replace a many-body heat bath (often modeled by an infinite collection of quantum Harmonic Oscillators) as a source of decoherence [3]. Other studies focused on entanglement generation: the rate of growth of the von Neumann entropy of the subsystem - ie the rate at which the subsystem becomes entangled with its environment - is directly related to measures of the chaos in the subsystem’s classical limit [4, 5, 6].

The chaos paradigm known as the Quantum Kicked Rotor (QKR) [7] plays a central role in these studies. The QKR corresponds to the dynamics of independent quantum particles evolving under the rather simple Hamiltonian $H_i = \frac{p_i^2}{2} + K \sin x_i \sum_n \delta(t - nT)$, where K represents the kick-strength and T the kick-period. Cold atoms in pulsed standing waves of light were found to provide a very clean realization of the QKR: in 1995, the phenomenon of the quantum suppression of classical chaotic diffusion was clearly demonstrated experimentally [8]; later, the recovery of the classical diffusive behavior in the presence of decoherence was also observed [9]. These works were followed by other studies by different experimental cold-atom groups worldwide [10] probing wide-ranging aspects of the QKR dynamics. In a previous work [11, 12], we proposed that the singly-excited Heisenberg spin-chain in a pulsed parabolic field could

provide an exact physical realization of the QKR: the dynamics of the spin-waves are given by a time-evolution operator of analogous form to that of the QKR.

Coupled QKR, have also been investigated in a number of theoretical studies, though, unfortunately, no physical realization has yet been achieved. In this case, one considers two QKR Hamiltonians with an additional coupling potential V , i.e. $H = H_1 + H_2 + V(x_1, x_2, t)$. In [13], interactions which depended on the separation of two rotors with a non-local sinusoidal term were investigated; in [14] the two particles were confined to within a short distance of each other. However, several studies considered a sinusoidal coupling term dependent on a center-of-mass coordinate, [15, 16, 17] such as e.g.: $V(x_1, x_2, t) = K_{12} \cos(x_1 + x_2) \sum_n \delta(t - nT)$.

In this work we show for the first time that the doubly-excited Heisenberg spin-chain system may-to a good approximation-be analyzed as pair of coupled kicked rotors. In fact, in this system, Nature even provides a coupling term of the centre-of-mass form $K_{12} \cos(x_1 + x_2)$. The mapping is, however, far less straightforward than that found for the one-excitation system in [11, 12]: the coupling here is mediated by bound-pair eigenstates (not found in the corresponding one-excitation chain), rather than spin waves, so acts only over a restricted part of the “image” phase-space. The wavenumbers of the bound states are complex, further complicating the mapping. Nevertheless, the analogy holds sufficiently well, so one can use it to shed insight on the dynamics. Further, it points to useful applications in state transfer, since we can use this understanding to control whether the two spin-flips propagate along the chain together, or separately. This adds to other applications that make use of the single-excitation correspondence [18].

In Section II we review briefly the one-particle dynamics of the Heisenberg XXZ spin chain and its mapping to the QKR. In section III we consider the doubly-excited spin chain. We summarize essential features of the well-known XXZ eigenstates and their dependence on the anisotropy parameter Δ . We then introduce the anal-

ogy with the two-particle coupled QKR and explore the dynamics when the initial state consists of two neighboring spin-flips. We also highlight two cases where the kicked rotor correspondence simplifies: i) when $\Delta = 0$ the kicked spin-chain can be mapped to a pair of independent QKRs; and ii) when $\Delta \gg 1$ the bound states effectively trap two excitations on neighboring sites and we show that in this limit, these bound states give rise to a further analogy with the QKR. We finish, in section IV with examples of how we can use these results to manipulate correlations in the spin-flip locations.

II. THE HEISENBERG SPIN-CHAIN AND ITS ONE-PARTICLE IMAGE

The well-known spin-1/2 Heisenberg XXZ chain is governed by the Hamiltonian:

$$H_{hc} = -\frac{J}{4} \sum_{n=1}^N \left(2(\sigma_n^+ \sigma_{n+1}^- + \sigma_n^- \sigma_{n+1}^+) + \Delta \sigma_n^z \sigma_{n+1}^z \right) - B \sum_n \sigma_n^z. \quad (1)$$

When investigating the dynamics of spin-chains such as this, a useful approach is to invoke quasi-particle models and interpret excited states as systems of indistinguishable particles. In some cases, it is even possible to map the dynamics to a one-body “image” system which approaches the classical limit as $N \rightarrow \infty$ [19].

H_{hc} conserves the number of spin-flips and a single excitation represents a spin-wave which distributes a single spin-flip throughout the chain. Higher excited-states correspond to multiple spin-waves which interact when they coincide through both an exclusion process (no two spin flips can simultaneously occupy the same site) as well as a mutual interaction induced by the $\sigma_n^z \sigma_{n+1}^z$ (Ising) term - the strength of which is determined by the anisotropy parameter Δ . Note that $\Delta = 0$ corresponds to the XX0 chain and $\Delta = 1$ is the isotropic Heisenberg chain.

The eigenstates for the single spin-flip sector of (1), spanned by the basis states $\{|n\rangle = \sigma_n^- |\uparrow \uparrow \dots \uparrow\rangle : n = 1, \dots, N\}$, are translationally invariant magnon states with momenta κ :

$$|\kappa\rangle = \frac{1}{\sqrt{N}} \sum_{n=1}^N e^{i\kappa n} |n\rangle. \quad (2)$$

Note that periodic boundary conditions are used, i.e. the configuration is a closed ring with $\sigma_{j+N}^\alpha = \sigma_j^\alpha$. The magnon momenta are determined by these conditions and take the values $\kappa = 2\pi I/N$, $I = 1, \dots, N$. These states have energy:

$$E - E_0 = 2B + J(\Delta - \cos \kappa), \quad (3)$$

where the ground state energy $E_0 = -J\Delta N/4$, i.e. $H_{hc} |\uparrow \uparrow \dots \uparrow\rangle = E_0 |\uparrow \uparrow \dots \uparrow\rangle$. Adding an external parabolic kicking field to the Heisenberg Hamiltonian

gives:

$$H = H_{hc} - \frac{B_Q}{4} \sum_{n=1}^N (n - n_0)^2 \sigma_n^z \sum_{j=1}^N \delta(t - jT), \quad (4)$$

where the kicking field has amplitude B_Q with minimum at n_0 . Time evolving the time-periodic H for one period T yields a unitary map,

$$|\psi(t = (j+1)T)\rangle = U(T) |\psi(t = jT)\rangle \quad (5)$$

where

$$U(T) = e^{-iTH/\hbar} = e^{i\frac{B_Q}{4\hbar} \sum_{n=1}^N (n-n_0)^2 \sigma_n^z} e^{-iTH_{hc}/\hbar} \quad (6)$$

since the δ -kick nature of the time-dependent field permits us to split the operators.

Using (2) and (3), it was shown in [11, 12], that the matrix elements of $U(T)$ in the single-flip basis $\{|n\rangle\}$ have a form very similar to the matrix used to evolve the quantum chaos paradigm, the QKR. These are given by:

$$U_{nn'} \simeq e^{i\frac{B_Q}{2}(n-n_0)^2} i^{n'-n} J_{n'-n}(JT) \quad (7)$$

for the spin-ring (an analogous form was given in [11] for open boundary conditions). Here, $J_n(x)$ denotes a Bessel function of order n and, for convenience, we have set $\hbar = 1$.

We recall the form of the QKR Hamiltonian:

$$H_{QKR} = \frac{\hat{p}^2}{2} - k \cos \hat{x} \sum_{j=1}^N \delta(t - jT). \quad (8)$$

with $x \in [0, 2\pi)$. In its classical limit, the dynamics is described by the famous Standard Map which is known to display a transition from integrability to chaos as the *Stochasticity Parameter*, $K = kT$, is increased. For $K \lesssim 1$ diffusion in momentum is blocked by invariant tori running through classical phase space. At large K phase space is almost completely chaotic and unbounded diffusion in momentum is typically seen. However, in certain ranges of $K \approx 2j\pi$, $j \in \mathbb{Z}$, small transporting islands known as “Accelerator Modes” (AM) appear in classical phase space and give rise to anomalous diffusion. In the QKR, diffusion of momentum at large K is suppressed by quantum interference in a process known as Dynamical Localization [20, 21]. We can express the QKR time propagator in a basis of plane waves $|l\rangle = \exp(ilx)$:

$$\langle l|U_{QKR}(T)|l'\rangle = e^{-il^2\tau/2} i^{l'-l} J_{l'-l}\left(\frac{K}{\tau}\right). \quad (9)$$

Here $\tau = \hbar T$ is the rescaled effective Planck’s constant.

Comparing the above with (7) we see that the QKR and spin-chain propagators are of similar form, provided we identify $\frac{K}{\tau} \rightarrow JT$ and note that the kicking field $B_Q \rightarrow \tau$ plays the role of an effective Planck’s constant. In effect, the spin-chain equivalent to the $K \cos x$ term

in H_{QKR} arises from the dispersion relation of the spin-waves, ie re-writing (1):

$$H_{hc} = \sum_{\kappa} J(\Delta - \cos \kappa) |\kappa\rangle \langle \kappa| \quad (10)$$

So, to make the QKR \rightarrow spin-wave mapping we also had to identify position (x) in the QKR, with momentum in the spin-chain (κ); and momentum in the QKR with position (spin-site) in the chain.

With the aid of this mapping we can identify the spin-wave equivalent of classical chaos phenomena such as Accelerator Modes (AM), transport on tori [22], cantori or stable islands, and quantum chaos phenomena like Dynamical Localization [7]. The classical transporting islands represented by the AM have evident potential applicability in quantum state transfer so, below, we investigate these in particular: they occur for $K \approx 2j\pi$ where j is an integer. In the classical image phase-space, they correspond eg to initial conditions located around $(x_0, p_0) \approx (\pm\pi/2, 0)$ which “hop” in momentum each period such that at $t = nT$ ($n \in \mathbb{Z}$):

$$(x_n, p_n) \approx (\pi/2, \mp 2\pi nj). \quad (11)$$

Quantum mechanically, if the effective Planck’s constant is small enough, these islands can support Gaussian states that follow the classical trajectories - i.e. they “hop” in momentum every period [23]. Gaussian excitations were indeed seen in the one-flip spin-chain, [11], provided the initial spin-flip occurs at a site near the minimum of the magnetic kicking field and $K = JTB_Q \approx 2\pi j$. The excitations were seen to hop approximately $2\pi/B_Q$ sites each period, with little dispersion.

We now consider the two-flip case.

III. TWO SPIN EXCITATIONS

A. Bound-pair states and spin-waves

Eigenstates in the double excitation sector are expressed, via the Bethe ansatz, as pairs of spin waves [24]:

$$|\kappa_1, \kappa_2\rangle = A(\kappa_1, \kappa_2) \sum_{0 \leq n_1 < n_2 \leq N} a(n_1, n_2) |n_1, n_2\rangle. \quad (12)$$

where $A(\kappa_1, \kappa_2)$ is a normalization constant. $|n_1, n_2\rangle$ denotes a state with a spin-flip at sites n_1 and n_2 . Bethe’s ansatz for the amplitude is

$$a(n_1, n_2) = e^{i(\kappa_1 n_1 + \kappa_2 n_2 + \theta/2)} + e^{i(\kappa_1 n_2 + \kappa_2 n_1 - \theta/2)}. \quad (13)$$

The scattering phase $\theta(\kappa_1, \kappa_2)$ accounts for the interaction between the pair of spin-waves. On applying H_{hc} in (1) to these states and solving the eigenvalue equations, one obtains the dispersion relation

$$E - E_0 = 4B + J(2\Delta - \cos \kappa_1 - \cos \kappa_2) \quad (14)$$

and also a relation between θ and the quasi-momenta, the Bethe Ansatz Equation (BAE):

$$e^{i\theta} = -\frac{1 + e^{i(\kappa_1 + \kappa_2)} - 2\Delta e^{i\kappa_1}}{1 + e^{i(\kappa_1 + \kappa_2)} - 2\Delta e^{i\kappa_2}} \quad (15)$$

Further restrictions are imposed by the periodic boundary conditions:

$$N\kappa_1 = 2\pi\lambda_1 + \theta, \quad N\kappa_2 = 2\pi\lambda_2 - \theta. \quad (16)$$

where the Bethe quantum numbers $\lambda_1 \leq \lambda_2$ are integers in the range $\lambda_i \in \{0, 1, \dots, N-1\}$. By solving the coupled system of equations in (15) and (16), $\kappa_{1,2}$ and θ can be obtained. Broadly speaking, these solutions fall into two groups depending on whether θ has an imaginary component. The majority of the solutions of (15) are real - these correspond states of two magnons which scatter off each other. For $\Delta = 0$ all the available solutions of (15) are real (and equal to π). When θ is complex, the eigenstates correspond to bound states of two spin flips. The probability amplitudes of these states are at a maximum when the flips are on neighboring sites and they decay exponentially with the separation of the flips. While for any given $\Delta \neq 0$ the widths of these states vary with the total momentum $\kappa_1 + \kappa_2$, they become narrower as Δ increases. Crucially, for long chains ($N \rightarrow \infty$) the energy of these states can be written [25]:

$$E - E_0 = 4B + J\Delta - \frac{J}{2\Delta}(1 + \cos(\kappa_1 + \kappa_2)). \quad (17)$$

when $\Delta > 0$.

B. Analogy with a pair of coupled kicked rotors

The departure point for our analysis of the spin dynamics as a system of coupled QKRs is the two-excitation spin-Hamiltonian, equivalent of (10):

$$\begin{aligned} H_{hc} = & \hat{P}_s \sum_{\kappa_{1,2}} J(\Delta - \cos(\kappa_1) - \cos(\kappa_2)) |\kappa_1, \kappa_2\rangle \langle \kappa_1, \kappa_2| \\ & - \hat{P}_b \sum_{\kappa_{1,2}} \frac{J}{2\Delta} (1 + \cos(\kappa_1 + \kappa_2)) |\kappa_1, \kappa_2\rangle \langle \kappa_1, \kappa_2| \\ & + \hat{\mathbb{I}}(E_0 + 4B + \Delta J) \end{aligned} \quad (18)$$

for $\Delta > 0$. Here \hat{P}_s is a projector on to the scattering-state component of Hilbert space, and \hat{P}_b onto the bound states.

Comparing the above with the typical coupled QKR potential $V(x_1, x_2) = K_1 \cos x_1 + K_2 \cos x_2 + K_{12} \cos(x_1 + x_2)$ and identifying $\kappa_i \rightarrow x_i$ and $K_{12} \rightarrow \frac{JT}{2\Delta}$ might suggest that the scattering states be interpreted as giving rise to a pair of kicked rotors; and that a coupling between these rotors arises due to the bound states. However, we note the important difference that the κ_i for the scattering and bound states correspond to complementary portions of the “image” phase space. For the bound states, κ_i is complex, but $(\kappa_1 + \kappa_2)$ is real. In addition, we show below (in (22)) that in fact, for large Δ , K_{12} , i.e. the effective coupling is twice as large as suggested by (18).

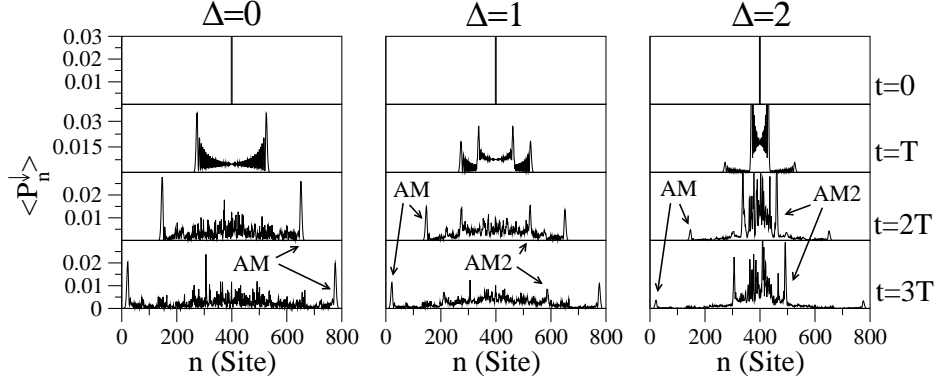


Figure 1: Showing the production of “bound state” accelerator modes (AM2) which move slowly, and fast “scattering state” accelerator modes (AM). When $\Delta = 0$ only the AM are present, in this case the dynamics maps to two independent QKRs. With increasing Δ the AM2 become dominant. We plot the on-site magnetization for two initially neighboring spin-flips $|\psi(0)\rangle = |400, 401\rangle$. We have chosen here, the parameters $K_s = 13$, $B_Q = 0.1$, $n_0 = 400$ and $T = 1$ for chains of 800 spins, which are known to produce Gaussian excitations in a singly-excited chain.

The parabolic kick will couple the eigenstates to each other (including coupling bound-pair and scattering states). As Δ increases, the overlap between the bound and scattering state energies decreases and the two bands separate for $\Delta > 2$. This will suppress the coupling and imply that for large Δ , if the initial state has negligible overlap with the bound subspace, the dynamics will be essentially uncoupled.

C. Evolution of $|n, n+1\rangle$ initial states

In this section, we explore the dynamics of an initial state prepared with two spin-flips localized on neighboring sites near the center of the chain $|\psi(0)\rangle \equiv |n_0, n_0+1\rangle$. Parameters corresponding to accelerator modes are used: $JT = 130$ and $B_Q = 1/10$, so $K \sim 4\pi$. Fig. 1 shows the resulting on-site magnetization $\langle P_n^\downarrow \rangle = \langle \frac{1}{2}(1 - \sigma_n^Z) \rangle$ of $|\psi(0)\rangle$ after successive applications of the map (6) for $\Delta = 0, 1$ and 2 .

When $\Delta = 0$, a pair of hopping wavepackets is produced. Each travels $2\pi/B_Q \approx 130$ sites each period. This is consistent with the single-particle accelerator modes (see previous section). In contrast, when $\Delta = 1$ or 2 , there are two sets of hopping wavepackets. One pair (AM) evolve like those in the $\Delta = 0$ chain, while the other pair (AM2) hop approximately $\pi/(\Delta B_Q)$ sites each period. For $\Delta = 1$ the AM2 wavepackets decay rapidly and by the third period ($t = 3T$) they are almost indistinguishable from the chaotic central portion.

To get a more complete picture of the dynamics we plot, in Fig. 2, the two-site correlation function $\langle P_{n_1}^\downarrow P_{n_2}^\downarrow \rangle$ for $|\psi(T)\rangle$, allowing us to follow the relative positions of the spin-flips. We find that the AM2 wavepackets contain flips that travel together, this suggests they are supported by the bound states. The AM wavepackets on the other hand appear in an anti-correlated portion of the wavefunction.

We now consider these two different kinds of behaviour in more detail.

D. $\Delta = 0$ and ‘independent’ QKRs

For $\Delta = 0$ only the exclusion interaction is present between flips. The effects of this interaction are subtle and sensitive to the initial conditions. For certain cases, where the flips are initially separated by an odd number of sites, it has been shown to change the character of entanglement when the two excitations collide [26]. A separate study on the transfer of entangled states in a doubly excited XX0 chain was carried out in [27].

Here, we are interested what influence the exclusion interaction has on the QKR-like behaviour of excitations in the kicked spin-chain. The $\Delta = 0$ model can be mapped to a system of spinless fermions via the Jordan-Wigner transformation (see appendix for details). The number of fermions matches the number of spin-flips. The exclusion interaction is accounted for by the anti-commuting property of the fermionic operators. Consequently, the fermions are “free” (non-interacting) and can be evolved separately under the single-particle dynamics. The result of this is that the kicked chain maps to a system of non-coupled QKRs. However, in the spin representation, the exclusion interaction is still relevant (the spin-flips do not evolve separately). To see this we make use of the Floquet operator in the two spin-flip basis (see appendix):

$$\begin{aligned} \langle n_1, n_2 | U^{\Delta=0}(T) | m_1, m_2 \rangle = & e^{-i \frac{B_Q}{2} [(n_1 - n_0)^2 + (n_2 - n_0)^2]} i^{n_1 + n_2 - m_1 - m_2} \times \\ & [J_{n_1 - m_1}(\beta) J_{n_2 - m_2}(\beta) - J_{n_1 - m_2}(\beta) J_{n_2 - m_1}(\beta)], \end{aligned} \quad (19)$$

where $\beta = JT$ and $N \rightarrow \infty$.

The effects of the exclusion interaction are not actually seen in Fig. 1. For example, the on-site magnetization after one period (i.e. for $|\psi(t = T)\rangle$) is

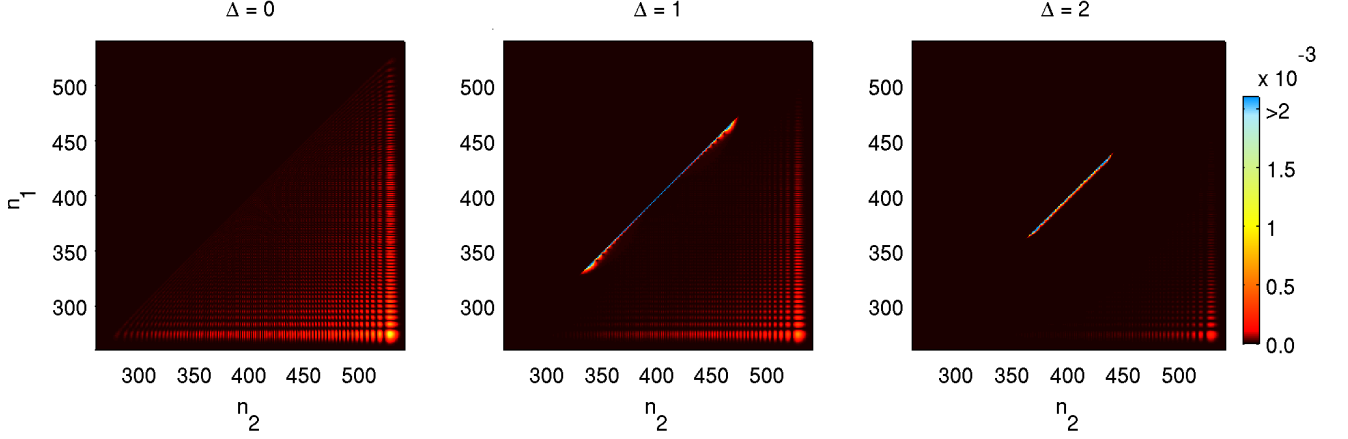


Figure 2: (color online) Spin-spin correlations corresponding to Fig. 1 at $t = T$. The two-site correlation function $\langle P_{n_1}^\downarrow P_{n_2}^\downarrow \rangle$, equal to the probability of finding one flip on site n_1 and the other on n_2 , is shown. At $\Delta = 0$ the spins are anti-correlated in contrast to Fig. 1 which suggests the dynamics of uncoupled particles. $\Delta = 1$ and 2 have an anti-correlated component (flips separate) as well as an additional component where the flips travel together.

$\langle P_n^\downarrow \rangle = \sum_{n_1 < n} |U_{n_1, n, n_0, n_0+1}^{\Delta=0}|^2 + \sum_{n_2 < n} |U_{n, n_2, n_0, n_0+1}^{\Delta=0}|^2$, which is $\langle P_n^\downarrow \rangle = J_{n-n_0}^2(\beta) + J_{n-n_0+1}^2(\beta)$. This is the same as for two independent spin-flips initialized at sites n_0 and $n_0 + 1$. Using the free-fermion correspondence, it is straightforward to show that for all later times $\langle P_n^\downarrow \rangle$ is exactly equivalent to the sum of expectations for a pair of uncoupled QKRs.

The coupling induced by the exclusion interaction is, however, evident in Fig. 2, which plots the two-site correlations after the first period: $\langle P_{n_1}^\downarrow P_{n_2}^\downarrow \rangle = |U_{n_1, n_2, n_0, n_0+1}^{\Delta=0}|^2$. Its effect, for this particular initial state, is to prevent the spin-flips from travelling together. The two site correlation is highest when the flips travel $JT = 130$ sites in opposite directions. If the flips were non interacting (i.e. allowed to co-exist on the same site) then it would be equally likely the flips would travel together or apart. Different correlations are seen when the initial separation of the flips is changed.

So when $\Delta = 0$, where the Heisenberg chain eigenstates consist entirely of scattering states, the behavior of two spin-flips is like that of two Kicked Rotors except the flips build up correlations in their relative positions.

E. Bound State QKRs for large Δ

When $\Delta \neq 0$, the spin-flips can form bound pairs, and when $\Delta = 1$ or 2, a pair of neighbouring spin-flips will overlap with both bound and scattering eigenstates. The additional features seen in the probability distributions when $\Delta = 1$ and 2 are remnants of QKR-like behavior of bound states that appears in the limit of large Δ . In this limit, the bound states confine the flips to neighboring sites. Santos and Dykman [28] use a perturbation expansion in spin coupling strength J to produce an ef-

fective Hamiltonian when $\Delta \gg 1$. In this approximation the bound state amplitudes are:

$$a(n_1, n_2) = \delta_{n_1, n_2-1} e^{i(\kappa_1 + \kappa_2)n_1} \quad (20)$$

and their dispersion relation remains unchanged from (17). Clearly, in center of mass coordinates, the bound states have the same form as a single magnon solution. Naturally, this similarity extends to the dynamics of states on the nearest neighbor (NN) subspace, $\{|n, n+1\rangle\}$: Two initially neighboring spin-flips evolve together in approximately the same way as a lone flip in the single excitation basis $\{|n\rangle\}$. We anticipate that for $\Delta \gg 1$:

$$\langle n_1, n_2 | U_{hc}(t) | m, m+1 \rangle \approx i^{n_1-m} J_{n_1-m} \left(\frac{Jt}{2\Delta} \right) \delta_{n_1, n_2-1} \quad (21)$$

where the propagation of the neighboring flips is slower than for a single flip - it is scaled by $J/(2\Delta)$ rather J .

The influence of the kicking field on the NN subspace can be incorporated into (21) to give:

$$\langle n_1, n_2 | U_H(T) | m, m+1 \rangle \approx \delta_{n_1, n_2-1} e^{iB_Q(n_1 - (n_0 - \frac{1}{2}))^2} i^{n_1-m} J_{n_1-m} \left(\frac{JT}{2\Delta} \right) \quad (22)$$

up to a global phase. Again, we see an analogy to a QKR, with stochasticity parameter $K_b = JT B_Q / \Delta$ and effective Planck's constant $\tau_b = 2B_Q$.

We expect the accuracy of this approximation to fall with decreasing Δ as the bound states become broader and are coupled more strongly to the scattering states by the kicking field. However, we show in Fig. 3 that even for $\Delta = 2$, QKR-like behavior is still seen on the NN subspace for short times.

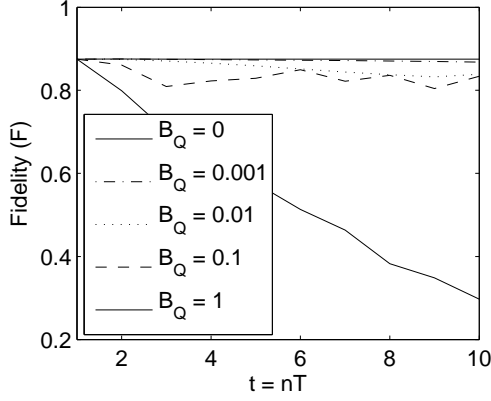


Figure 3: Showing the decay, over time, of the correspondence between the dynamics of nearest neighbor flips and a QKR. F is the fidelity of the time evolution of two spin-flips initially on neighboring sites $|\psi(t = nT)\rangle = [U(T)]^n |100, 101\rangle$ to the matrix elements (21) and (22) for various B_Q and $JT/\Delta = 5$, $\Delta = 2$.

F. Scattering State QKRs and Center of Mass Diffusion

We now consider parameter ranges for which a single particle displays Dynamical Localization. Taking $K = JTB_Q = 5.0$ and $B_Q = 1$ a lone flip initially spreads diffusively but at long times this spreading saturates and the flip becomes exponentially localized $\langle P_n^\downarrow \rangle \sim \exp\{-2|n - n_{\text{init}}|/L\}$ with a localization length $L = (JT)^2/4$. The diffusion time is usually increased for coupled kicked rotors, e.g. in a related study [29] a pair of rotors coupled locally in momentum $U\delta p_1, p_2$ were shown to localize with a much greater L .

In Fig. 4 we follow the center of mass spreading of two spin-flips using the second moment $\langle (n_1 + n_2 - 2n_0)^2 B_Q^2 \rangle$. The flips are initialized 10 sites apart so in the limit of large Δ this state should overlap only with scattering states. The spin-distribution localizes for $\Delta = 0$ as expected for an uncoupled QKR; however, for larger Δ , the diffusion is not halted, but slows down appreciably after the “break-time” at $\Delta = 0$. This slower diffusion saturates and reaches a constant rate for $\Delta \gtrsim 1$.

For large Δ , due to the large energy gap, the kicking field will not significantly couple the bound and scattering states so the quantum state is supported only by the scattering states for all time. The behavior of the diffusion however, does not reduce to that of uncoupled kicked rotors (as might be suggested by the dispersion relation in (18)). This is because the scattering states do not exactly reduce to a pair of magnons-even in the large N limit where the corrections to the momenta $\kappa_{1/2}$ (see (16)) vanish (i.e. $\theta/N \rightarrow 0$). They are distorted by the Ising term and correspondingly the presence of the bound states. This can be seen by rearranging the Bethe equations in section A. For $\Delta \neq 0$ the scattering state

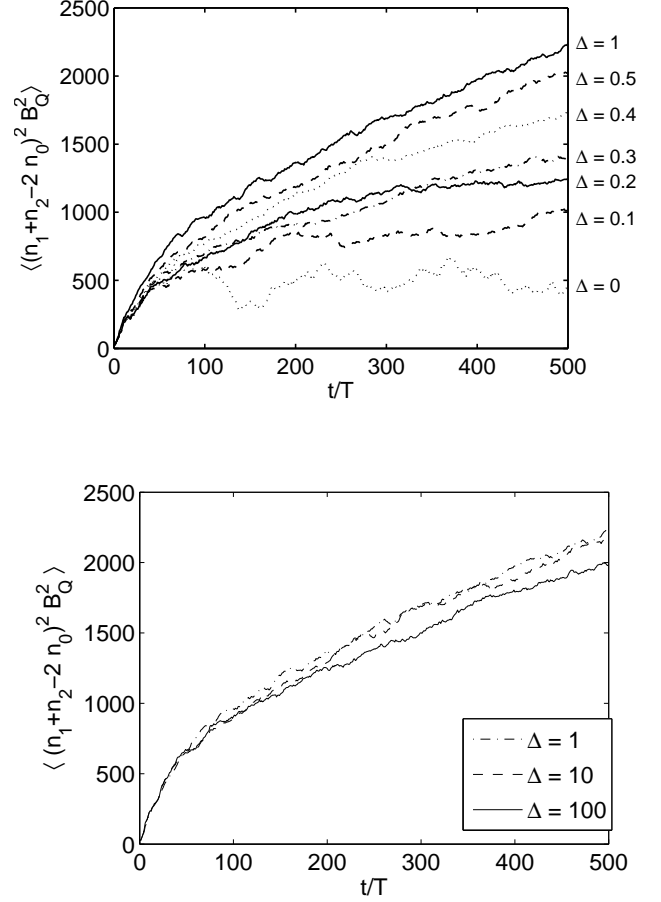


Figure 4: Influence of the $\sigma_i^z \sigma_{i+1}^z$ coupling on the growth of the ‘center of mass’ second moments for two flips initialized 10 sites apart and parameters $K = 5$ and $B_Q = 1$ on a chain of 200 spins.

amplitudes can be written

$$a(n_1, n_2) \propto e^{i \frac{\kappa_c}{2} (n_1 + n_2)} \left[\sin(\kappa_r (n_1 - n_2 + 1)) - \frac{\cos \frac{\kappa_c}{2}}{\Delta} \sin(\kappa_r (n_1 - n_2)) \right] \quad (23)$$

where $\kappa_c = 2\pi(\lambda_1 + \lambda_2)/N$ and $\kappa_r = (\pi(\lambda_1 - \lambda_2) + \theta)/N$. Notably, when $\Delta \gg 1$, the scattering states typically have no overlap with the $|n, n+1\rangle$ subspace (except, eg, for the $\lambda_1 = \lambda_2 = \theta = 0$ state) as this is occupied by the bound states.

IV. POSSIBILITIES FOR CONTROLLING THE EVOLUTION OF SPIN-FLIPS

These results may be of interest in the context of quantum information and state transfer as they suggest possibilities for manipulating the evolution of spin-flips (and spin-correlations) in a Heisenberg chain. Clearly, the evolution of a two-particle state on the non-kicked

XXZ chain depends on Δ and the shape of the initial wavepacket. These two factors also determine the proportion of the wavefunction that is supported by the scattering/bound states. In the kicked chain, for large Δ , the scattering and bound states correspond to different QKR images: The bound (b) and scattering state (s) QKR image parameters are related via $K_b = K_s/\Delta$ and $\tau_b = 2\tau_s$. So, by picking suitable values of JT and B_Q we can select which dynamical regimes the bound and scattering components correspond to.

For example, one could halt the propagation of either the bound or scattering state portion of the wavefunction and allow the rest to travel. A possible way to do this is to make use of resonances in the QKR. These occur for $\tau = 4\pi r$ where r is rational. For $r = 1$ (primary resonance) ballistic spreading occurs in momentum for the QKR (position for the spin chain) and when $r = 1/2$ (antiresonance) diffusion in momentum can be suppressed. These two conditions could be achieved for the bound and scattering states respectively by setting $\tau_b = 4\pi$. This would lead to ballistic diffusion for initially neighboring flips and could prevent flips that are initially well separated from spreading.

V. CONCLUSIONS

We have investigated the dynamics of a pair of spin-flips on a periodically kicked Heisenberg chain, focusing on the roles of the scattering and bound eigenstates of the underlying time independent model. Analogies to coupled and independent rotor systems have been identified and analysed.

T. B. acknowledges support from the EPSRC. This work was partly supported by Grant-in-Aid by MEXT, Japan.

Appendix A: TIME EVOLUTION FOR THE KICKED XX0 MODEL

Here, we show how the kicked XX0 chain (obtained from (4) by setting $\Delta = 0$) maps to a system of independent QKRs. This is done by first applying the Jordan-Wigner transformation [30], a non-local mapping of spin-flips on the chain to free fermions on a lattice. This transformation defines fermion creation and annihilation operators, c_j^\dagger and c_j respectively, in terms of spin operators so that $\sigma_i^z = (1 - 2c_i^\dagger c_i)$ and

$$\hat{\sigma}_i^+ = \left[\prod_{j < i} (1 - 2c_j^\dagger c_j) \right] c_i, \quad \hat{\sigma}_i^- = \left[\prod_{j < i} (1 - 2c_j^\dagger c_j) \right] c_i^\dagger. \quad (\text{A1})$$

The product of $(1 - 2c_j^\dagger c_j)$ terms accounts for the difference between inter-particle exchange statistics - negative for fermions and positive for spin-flips. The creation and annihilation operators obey the standard commutation relations: $\{c_i, c_j^\dagger\} = \delta_{i,j}$ and $\{c_i, c_j\} = 0$ and are defined with respect to a vacuum state $|\phi\rangle$ such that $c_j|\phi\rangle = 0$.

Making use of the transformation and setting $\Delta = 0$, the kicked spin-chain Hamiltonian (4) becomes:

$$H = -\frac{J}{2} \left[\sum_{j=1}^{N-1} (c_j^\dagger c_{j+1} + c_{j+1}^\dagger c_j) - (-1)^r (c_1^\dagger c_N + c_N^\dagger c_1) \right] + \frac{B_Q}{2} \sum_{j=1}^N (j - j_0)^2 (1 - 2c_j^\dagger c_j) \delta(t/T). \quad (\text{A2})$$

The transformed Hamiltonian has boundary terms that depend on whether the number of fermions, r , is odd or even; these arise from the periodic boundary conditions $\sigma_{N+1}^\pm = \sigma_1^\pm$ and $\sigma_{N+1}^Z = \sigma_1^Z$.

We now calculate the result of time evolving over one period. Using the Heisenberg picture, we define $c_j^\dagger(T) = U^\dagger(T) c_j(0) U(T)$, where $U(T)$ is the Floquet operator of eq. 6. The absence of any mutual interaction (i.e. terms of the form $v(j_1 j_2, j'_1 j'_2) c_{j_1} c_{j_2} c_{j'_1}^\dagger c_{j'_2}^\dagger$) in (A2) implies the fermions are “free” and therefore the fermion operators can be time evolved using single particle states: $U^\dagger(T) c(\psi(0)) U(T) = c^\dagger(\psi(-t))$ where $c^\dagger(\psi(-t))$ creates the single particle state $\psi(-t) = U^\dagger(T) \psi(0)$. This corresponds to the single-flip basis, so $c_j^\dagger(T)|\phi\rangle = U^\dagger(T)|j\rangle$. Using the matrix elements $U_{nn'}$ in (7) gives, up to a global phase,

$$c_j^\dagger(T) \approx e^{iB_Q(j-j_0)^2/2} \sum_{j'} i^{j'-j} J_{j'-j}(-JT) c_{j'}^\dagger(0). \quad (\text{A3})$$

The equivalence between this propagator and the time-evolution for the QKR is clear and the parameters correspond as before: $JTB_Q \rightarrow K$ and $B_Q \rightarrow \tau$. Therefore, a kicked fermion evolves in position in the same way as a QKR evolves in momentum i.e. $j \rightarrow l\tau$. This multiple-fermion correspondence is a direct extension of the single-flip analysis [11, 12].

Calculating two-particle correlation functions is now straightforward. For example, we find the matrix element of the Floquet operator in the two spin-flip basis $|n_1, n_2\rangle = -c_{n_2}^\dagger c_{n_1}^\dagger |\phi\rangle$,

$$\begin{aligned} \langle n_1, n_2 | U(T) | m_1, m_2 \rangle &= \langle \phi | c_{n_1} c_{n_2} U(T) c_{m_1}^\dagger c_{m_2}^\dagger | \phi \rangle \quad (\text{A4}) \\ &= \left(\langle \phi | c_{m_1} c_{m_2} c_{n_2}^\dagger(T) c_{n_1}^\dagger(T) | \phi \rangle \right)^*. \end{aligned}$$

Substituting (A3) into this

$$\begin{aligned} \langle n_1, n_2 | U(T) | m_1, m_2 \rangle &= \sum_{i_1, i_2} e^{-i\frac{B_Q}{2}[(n_1-j_0)^2 + (n_2-j_0)^2]} \times \\ &\quad i^{i_1+i_2-n_1-n_2} J_{i_1-n_1}(-JT) J_{i_2-n_2}(-JT) \times \\ &\quad \langle \phi | c_{m_1} c_{m_2} c_{i_2}^\dagger c_{i_1}^\dagger | \phi \rangle. \quad (\text{A5}) \end{aligned}$$

From Wick's theorem $\langle \phi | c_{m_1} c_{m_2} c_{i_2}^\dagger c_{i_1}^\dagger | \phi \rangle = \delta_{m_1, i_1} \delta_{m_2, i_2} - \delta_{m_1, i_2} \delta_{m_2, i_1}$ and therefore,

$$\begin{aligned} \langle n_1, n_2 | U(T) | m_1, m_2 \rangle &= e^{-i\frac{B_Q}{2}[(n_1-j_0)^2 + (n_2-j_0)^2]} \times \\ &\quad i^{n_1+n_2-m_1-m_2} [J_{m_1-n_1}(-JT) J_{m_2-n_2}(-JT) \\ &\quad - J_{m_1-n_2}(-JT) J_{m_2-n_1}(-JT)]. \quad (\text{A6}) \end{aligned}$$

Substituting $J_j(-\beta) = J_{-j}(\beta)$ into this yields (19).

Finally, we note that when $\Delta \neq 0$ the Ising term, $H_{ZZ} = -J\Delta \sum_n \sigma_n^Z \sigma_{n+1}^Z / 4$, introduces a mutual interaction between the fermions:

$$H_{ZZ} = J\Delta \sum_{j=1}^N c_j^\dagger c_j - \mathbb{I}/4 - c_j^\dagger c_{j+1}^\dagger c_{j+1} c_j. \quad (\text{A7})$$

As a result, the corresponding QKR images will be coupled.

-
- [1] W.H. Zurek, Rev. Mod. Phys. **75**, 715 (2003).
 - [2] G. Benenti, G. Casati, and G. Strini, *Principles of Quantum Computation and Information*, Vol 2 (World Scientific, 2007).
 - [3] D. Rossini, G. Benenti, and G. Casati, Phys. Rev. E **74**, 036209 (2006).
 - [4] W.H. Zurek and J.P. Paz, Phys. Rev. Lett. **72**, 2508 (1994).
 - [5] P.A. Miller and S. Sarkar, Nonlinearity **12**, 419 (1999).
 - [6] P.A. Miller and S. Sarkar, Phys. Rev. E **60**, 1542 (1999).
 - [7] G. Casati, B.V. Chirikov, F.M. Izraelev and J. Ford, Lect. Notes in Phys. **93** (Springer-Verlag, New York, 1979) p334.
 - [8] F. Moore, J.C. Robinson, C. Bharucha, B. Sundaram, and M.G. Raizen, Phys. Rev. Lett. **75**, 4598 (1995); M.G. Raizen, Adv. At. Mol. Opt. Phys. **41**, 43 (1999).
 - [9] H. Ammann, R. Ray, N. Christensen and I. Shvarchuck, J. Phys. B **31**, 2449 (1998).
 - [10] P. Szriftgiser, J. Ringot, D. Delande, J.-C. Garreau, Phys. Rev. Lett. **89**, 224101 (2002); P.H. Jones, M. Stocklin, G. Hur, and T.S. Monteiro, Phys. Rev. Lett. **93**, 223002 (2004); C. Ryu, M.F. Andersen, A. Vaziri, M.B. d'Arcy, J.M. Grossman, K. Helmerson, and W.D. Phillips, Phys. Rev. Lett. **96**, 160403 (2006); M. Sadgrove, M. Horikoshi, T. Sekimura, and K. Nakagawa, Phys. Rev. Lett. **99**, 043002 (2007); I. Dana, V. Ramareddy, I. Talukdar and G. S. Summy, Phys. Rev. Lett. **100**, 024103 (2008); J. F. Kanem, S. Maneshi, M. Partlow M. Spanner and A. M. Steinberg Phys. Rev. Lett. **98**, 083004 (2007).
 - [11] T. Boness, S. Bose and T.S. Monteiro, Phys. Rev. Lett. **96**, 187201 (2006).
 - [12] T. Boness, M. Stocklin and T.S. Monteiro, Prog. Theor. Phys. Suppl. **166**, 85 (2007).
 - [13] S. Adachi, M. Toda and K. Ikeda, Phys. Rev. Lett. **61**, 659 (1998); H. Fujisaki, A. Tanaka and T. Miyadera, J. Phys. Soc. Jpn. Suppl. C **72**, 111 (2003).
 - [14] H.K. Park and S.W. Kim, Phys. Rev. A **67**, 060102 (2003).
 - [15] A. Lakshminarayan, Phys. Rev. E **64**, 036207 (2001).
 - [16] B.P. Wood, A.J. Lichtenberg, and M.A. Lieberman, Physica D **71**, 132 (1994).
 - [17] S. Nag, G. Ghosh and A. Lahiri, Physica D **204**, 110 (2005).
 - [18] J. Gong and P. Brumer, Phys. Rev. A **75**, 032331 (2007).
 - [19] T. Prosen, Phys. Rev. E **60**, 1658 (1999); Phys. Rev. E **65**, 036208 (2002).
 - [20] S. Fishman, D.R. Grempel and R.E. Prange, Phys. Rev. Lett. **49**, 509 (1982).
 - [21] D.R. Grempel, R.E. Prange and S. Fishman, Phys. Rev. A **29**, 1639 (1984).
 - [22] K. Kudo and T.S. Monteiro, Phys. Rev. E **77**, 055203(R) (2008).
 - [23] J.D. Hanson, E. Ott, and T.M. Antonsen, Phys. Rev. A **29**, 819 (1984).
 - [24] H. Bethe, Z. Phys. **71**, 205 (1931); M. Karbach and G. Mller, Computers in Physics **11**, 36 (1997).
 - [25] M. Takahashi, *Thermodynamics of One-Dimensional Solvable Models*, Cambridge (2005).
 - [26] L. Amico, A. Osterloh, F. Plastina, R. Fazio and G.M. Palma, Phys. Rev. A **69**, 022304 (2004); L. Amico, R. Fazio, A. Osterloh and V. Vedral, Rev. Mod. Phys. **80**, 517-576 (2008).
 - [27] V. Subrahmanyam, Phys. Rev. A **69**, 034304 (2004).
 - [28] L.F. Santos and M.I. Dykman, Phys. Rev. B **68**, 214410 (2003).
 - [29] D.L. Shepelyansky, Phys. Rev. Lett. **73**, 2607 (1994).
 - [30] P. Jordan and E. Wigner, Z. Phys. **47**, 631 (1928); E. Lieb, T. Schultz and D. Mattis, Ann. Phys. **16**, 406 (1961).